FAST AND SELECTIVE MRI OF XENON BIOSENSORS

Martin Kunth[1], Jörg Döpfert[1], Christopher Witte[1], Federica Rossella[1], and Leif Schröder[1]
[1]*Leibniz-Institut für Molekulare Pharmakologie (FMP), Berlin, Germany*

Introduction: A method of increasing the detectable magnetization by a factor of >10,000 is spin-exchange optical pumping (SEOP) [1,2] for producing hyperpolarized (HP) xenon-129 (Xe). Xenon can be used as a functionalized solution state contrast agent by trapping it in host molecules such as cryptophane-A (CrA) cages [3]. These allow chemical exchange of xenon between the solution pool and xenon inside the cage. When xenon enters the cage, it changes its resonance frequency which can be directly detected, or at much lower concentrations indirectly detected using chemical exchange saturation transfer (CEST) [4]. This further increases the sensitivity up to three orders of magnitude. The combination of both enhancement strategies, coined Hyper-CEST [5], merges these benefits. However, the imaging of hyperpolarized nuclei is challenging, since each radio frequency excitation pulse depletes the hyperpolarization resulting in decreased signal. To overcome this problem, various techniques [6-8] have been proposed for other HP applications, but have not yet been implemented for Xe biosensors due to limited signal from dissolved Xe (Xe@solution). In this work, we combined echo-planar imaging (EPI) readout with a magnetization transfer module to perform EPI-Hyper-CEST and to image the spatial distribution of CrA agents with a concentration in the micro molar regime. By employing this fast imaging technique, the acquisition speed is no longer mainly limited by the image recording process as in the original approach [5], but mostly by the HP Xe delivery process. Our method turns out to be promising for fast biosensor detection even in the nanomolar range.

Material and methods: All experiments were performed on a 9.4 T NMR spectrometer. Fig. 1 shows the experimental setup of the double phantom consisting of an inner (IC - blue) and an outer compartment (OC - red). The IC contained cryptophane-A monoacid at a concentration of 10 µM in a solution of 10% Vol. DMSO and 90% Vol. H_2O (CrA1), the OC contained cryptophane-A monoacid at a concentration of 10 µM in a solution of 20% Vol. DMSO and 80% Vol. H_2O (CrA2). The different concentrations of DMSO cause a chemical shift difference between Xe inside CrA1 (Xe@CrA1) and Xe inside CrA2 (Xe@CrA2) as well as for the different Xe solution peaks. Using this effect, the chemical shift between Xe@CrA1 and Xe@CrA2 was adjusted to be about 1.2 ppm which simulates the behaviour of two potentially "different" biosensors.
To prove selectivity, a selective presaturation was combined with an EPI readout. Before each saturation (continuous wave (cw) pulse of 4s, B_1 = 1 µT) at a different frequency, fresh hyperpolarized Xe from a custom designed polarizer in continuous-flow mode was bubbled for 20 seconds into the sample. In order to allow all bubbles to collapse, a waiting time of 8 seconds was introduced. The EPI was employed using double sampling [9] and partial-Fourier acceleration by a factor of 1.68 resulting in 3 overscan lines. Therefore the encoding matrix was 32x19 to cover a field of view of 2x2 cm² yielding an acquisition time of 19.3 ms per image. Including the saturation time a total acquisition time of 4 seconds per image was achieved. The effective echo time was 5.7ms.

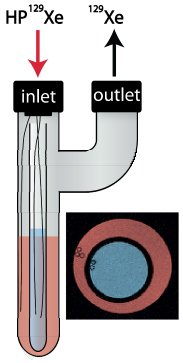

Fig. 1: Bubbling double phantom containing five capillaries (two in the IC and three in the OC). The FLASH image shows the axial slice of the phantom including the five capillaries.

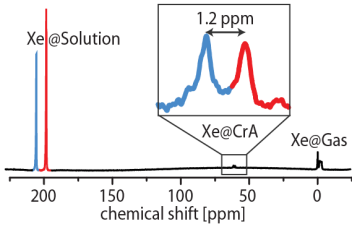

Fig. 2: Direct NMR spectrum of the sample. The peaks drawn in blue and in red correspond to the IC and OC, respectively. The chemical shift between Xe@CrA1/2 was adjusted to be 1.2 ppm.

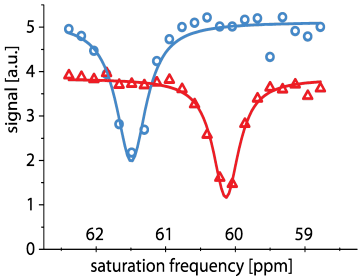

Fig. 3: z-Spectra of Xe@CrA1/2: The mean values within a region-of-interest for each offset frequency of the image stack from Fig. 2 is shown for the IC in blue and the OC in red.

Results and discussion: The NMR spectrum after 90° block pulse excitation with 16 averages is shown in Fig. 2 including a zoom of the Xe@CrA1/2 signal. The remaining z-magnetization was imaged 21 times after saturating at different frequencies around the Xe@CrA resonances (Fig. 4). The mean signal within a drawn region of interest for each compartment yields a z-spectrum as shown in Fig. 3.
The results show that even for low concentrations the two cage resonances with a chemical shift difference of only 1.2 ppm can be clearly separated by the proposed technique. The image contrast can be selectively changed by turning on/off different saturation pulses. A typical cartesian EPI-like chemical shift artifact occurs for different Xe@solution peak frequencies, which depends on the bandwidth (BW) of the k-space data points and is notable only in the phase direction (phase direction: BW = 1563 Hz => displacement ~16 pixel). Note that this will not appear for different cages in the same solvent. Previous studies that used 300 µM cryptophane achieved a SNR of 10 using a fast gradient echo pulse sequence with a voxel size of 117x125 µm² for one image in 25 s [10]. Our approach yields one image with SNR = 3–6 (10 µM CrA concentration respectively, SNR depending on DMSO fraction) and voxel size of (625 µm)² within 4 s being an acquisition time acceleration of ~6 although cage and xenon concentration is much lower. Our fast method demonstrates the possibility of single-shot localization of functionalized xenon as used in highly specific biosensors.

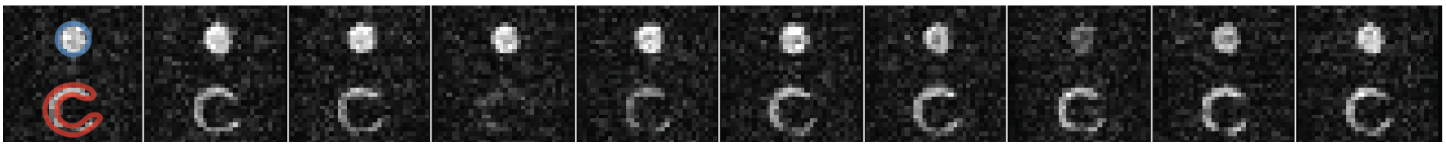

Fig. 4: Selected ^{129}Xe EPI images from the whole image stack for different saturation frequency offsets. In the first image the region-of-interests are shown for the IC in blue and for the OC in red.

References: [1] Happer, W.; *Rev. Mod. Phys.* 44:169–249 (1972), [2] Walker, T.G.; *Rev. Mod. Phys*. 69:629–642 (1997), [3] Spence et al.; *Proc. Natl. Acad. Sci.* 98:10654–10657 (2001), [4] Ward, K et al.; *Magn. Reson. Med.* 44:799–802 (2000), [5] Schröder, L et al.; *Science* 314:446–449 (2006), [6] Zhao, L.; *J. Magn. Reson. B* 113:179–183 (1996), [7] Deppe, M.H.; *Magn. Reson. Med.* – in press (2011), [8] Mansson, S et al.; *Acad.Rad.* 43:455–460 (2002), [9] Yang et al.; *J. Magn. Reson. B* 113:145–150 (1996), [10] Berthault, P et al.; *J. Am. Chem. Soc.* 130:16456–16457 (2008)